System reliability evaluation of in-service cable-stayed bridges subjected to cable degradation

Naiwei Lu [a*]; Yang Liu [a]; Michael Beer [b]

a. School of Civil Engineering, Changsha University of Science and Technology, Changsha Hunan 410114, China.

b. Institute for Risk and Reliability, Leibniz Universität Hannover, Hannover, Hannover 31509, Germany

* Corresponding author: Dr. Naiwei Lu, Email: lunaiweide@163.com

Biographical notes:

Naiwei Lu is a lecturer at Changsha University of Science and Technology, China. He received his Ph.D. (2015) from Changsha University of Science and Technology, China. He was a postdoctoral researcher (2016) in the Institute for Risk and Reliability at Leibniz University Hannover, Germany. His research interests are in reliability assessment of long-span bridges.

Yang Liu is a Professor of Civil Engineering at Changsha University of Science and Technology, China. He received his Ph.D. (2005) from Hunan University, China. His research interests are in bridge safety control and reliability assessment. Email: liuyangbridge@163.com

Michael Beer is a professor in the Institute for Risk and Reliability at Leibniz Universität Hannover, Germany. He is also a guest professor at the University of Liverpool and the Tongji University. He received his Ph. D. (2001) from Dresden University of Technology, Germany. His research interests are in uncertainty quantification and reliability assessment in civil engineering. Email: beer@irz.uni-hannover.de

System reliability evaluation of in-service cable-stayed bridges subjected to cable degradation

Abstract: The cables in a cable-stayed bridge are critical components supporting the long-span girders and ensuring their functionality. However, cables are prone to fatigue damage and atmospheric corrosion, which directly affect the bridge safety. This study presents a framework for system reliability evaluation of in-service cable-stayed bridges subjected to cable degradation. The effect of cable strength degradation on the bridge reliability is demonstrated through simulation on a parallel-series system representation. Machine learning techniques are utilized to approximate the nonlinear and dynamic response surfaces of critical components due to cable rupture, and the system reliability is finally evaluated from the event tree established by the β-unzipping method. Both short-span and long-span cable-stayed bridges are selected as prototypes to investigate the influence of cable degradation on the structural system reliability. On this basis it is revealed that cable degradation can significantly influence the collapse mechanism of a cable-stayed bridge and thereby lead to a significant reduction in the structural system reliability. This phenomenon is discussed in dependence on the cable spacing. Based on this effect, it is demonstrated that the consideration of cable corrosion and correlation is essential for lifetime safety evaluation of in-service cable-stayed bridges.

Keywords: cable-stayed bridge; cable degradation; corrosion; system reliability; failure path

1 Introduction

The cables in a cable-stayed bridge connecting bridge decks and pylons are critical components ensuring the long-span capability of bridge girders. The cables provide high degrees of redundancy for the structure, thereby making the

structural system stronger and more robust. However, cables are particularly vulnerable to fatigue damage and atmospheric corrosion during the service period (Li et al. 2012a; Yang et al. 2013), which can contribute to the risk of the bridge failure. In practice, fatigue damage and corrosion are normal phenomena for steel strands or parallel wires in a stay cable. An inspection conducted by Mehrabi et al. (2010) showed that 39 of the 72 cables of the Hale Bogges Bridge were critically in need of repair or replacement after a 25-year service period. Although a cable-stayed bridge is designed with enough conservatism, the system is still vulnerable due to cable degradation. The uncertainties in structural parameters also contribute to the system safety risks. Therefore, the influence of cable degradation on the system safety of cable-stayed bridges and the associated uncertainties deserves investigation.

The most evident form of cable degradation is the nonuniformly distributed reduction in the cross-sectional area of a cable due to environmental corrosion (Cao et al. 2003). The loss in cable cross-sectional area directly decreases the ultimate strength of a cable in a series-parallel system (Xu and Chen 2013). In addition to the continuous reduction in cable strength, cable degradation also increases the risk of cable rupture. During a cable rupture, the dynamic forces acting on the remaining system can lead to the overloading or failure of the adjacent cables and girders (Wolff and Starossek, 2009). This phenomenon has been summarized in terms of progressive collapse (Marjanishvili 2004) or

zipper-type collapse (Starossek 2007). To avoid the propagation of cable loss in a cable-stayed bridge, existing cable-stayed bridges are mostly designed with high degrees of static indeterminacy and conservatism (Aoki et al. 2013). However, the effects of cable loss on bridge safety, e.g., vehicle-bridge-wind interaction (Zhou and Chen 2014; 2015) and dynamic amplification factors (Mozos and Aparicio 2010), still attract the attention of researchers.

Since a cable provides a degree of redundancy for a cable-stayed bridge, the bridge failure can be defined as several components connected in series or in parallel. Taking into account uncertainties in the structural parameters, the structural safety evaluation of cable-stayed bridges subjected to cable degradation is more complicated. Stewart and Al-Harthy (2008) indicated that a spatial variability in corrosion of a steel bar led to a 200% higher failure probability. Research on the component-level reliability evaluation of cable-stayed bridges has got more progress, e.g. Chen and Xiao (2005) and Li et al. (2012). However, a cable-stayed bridge is a complicated system composed of multiple components, and the failure mode of the bridge is associated with numerous components. Hence, system reliability theory is appropriate for this issue (Estes and Frangopol 2001). The most influential approaches are the β-unzipping method (Thoft-Christensen and Murotsu 1986), the branch-and-bound method (Lee and Song, 2011), and the selective searching approach (Kim et al. 2013). Initially, Bruneau (1992) identified 9 potential failure patterns of a short-span cable-stayed bridge via the global

ultimate capacity approach. Li et al. (2010) utilized the β-unzipping method to evaluate the system reliability and found that the cables are the critical components impacting the system reliability of a cable-stayed bridge. Zhu and Wu (2011) utilized the Bayesian updating method to evaluate the system reliability of a cable-stayed bridge with inspection information. To make the computation more efficient, Lu et al. (2015) and Liu et al. (2016a) developed an adaptive support vector regression (ASVR) approach for system reliability evaluation of complex structures and applied it to cable-stayed bridges. Jia et al. (2016) utilized a direct differential method in a stochastic finite element model to simulate the response gradient of the structural system of a cable-stayed bridge. However, to the best of the authors' knowledge, research on system reliability evaluations of cable-stayed bridges subject to cable degradation remains limited.

This study aims to evaluate the system reliability of in-service cable-stayed bridges subjected to cable degradation. Strength reduction of parallel wire cables due to fatigue damage and corrosion are considered in a parallel-series system. An intelligent machine learning approach is presented for formulating the structural failure paths and evaluating the lifetime system reliability of cable-stayed bridges. Finally, two cable-stayed bridges, including an ancient short-span bridge and a modern long-span bridge, are selected as prototypes to investigate the influence of cable degradation on the structural failure modes and failure paths. Parametric studies associated with random variables and correlation coefficients are

conducted.

2 Strength reduction modeling of parallel wire cables

Both parallel wires and strands are conventional types of stay cables for a cable-supported bridge. A parallel wire cable consists of parallel, straight, round wires inside a polystyrene pipe. In addition to the material characteristics, the strength of parallel wires is also associated with the length and the number of wires (Nakamura and Suzumura 2012).

2.1 Effects of cable length and number of wires

First, this study conducts mathematical properties modeling of wire cables considering the effect of wire length and number of wires. In general, a parallel wire cable can be modeled in a series-parallel system, as shown in Fig. 1, where L and L_0 are total length and correlation length of the wire, respectively. In Fig. 1, each wire can be simulated as a series system, and the wires work together as a parallel system. In the series system, the individual wires of a stay cable can be simulated with correlative elements depending on the length of the wire. The material properties and defects in the wires are considered by a correlation length L_0 in the series system. The cable strength decreases in association with shorter correlation lengths or longer wire lengths. Therefore, both the correlation length and the wire length have been considered in the parallel-series model. A distribution function of the strength of a wire can be written using a Weibull cumulative distribution function (Weibull 1949):

$$F_z(z) = 1 - \exp\left[-\lambda\left(\frac{z}{u}\right)^k\right]$$ (1)

where z is the strength of a wire, λ is a scale factor describing the ratio between the length of the wire specimen and the correlation length, and u and k are unknown scale and shape parameters in the Weibull distribution function that can be estimated from ultimate capacity tests via the maximum likelihood method. An experimental study of a wire (L=100 m) conducted by Faber et al. (2003) indicated that the mean values of the wire strength for undamaged cable (λ=3) and corroded wire (λ=200) were 1748 MPa and 1650 MPa, respectively. The variability in the wire strength is negligible according to Faber's conclusions.
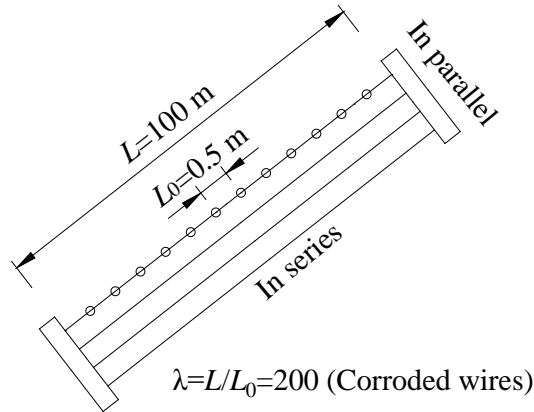

Fig. 1. A parallel- series system of a stay cable

In addition to the series system of an individual wire, a stay cable consists of numerous wires in parallel, as shown in Fig. 1. In the parallel system, increasing the number of wires (n) in a cable will reduce the mean strength of each wire, which is the so-called Daniel's effect (Daniels 1945). If n is large enough, the strength of a parallel wire follows a normal distribution with the mean value and standard deviation (Faber et al. 2003)

$$E(n) = nx_0(1 - F_Z(x_0)) + c_n \tag{2a}$$

$$D(n) = x_0 \left[nF_Z(x_0)(1 - F_Z(x_0)) \right]^{1/2} \tag{2b}$$

where, $c_n = 0.966an^{1/3}$, $a^3 = \dfrac{f_Z^2(x_0)x_0^4}{(2f_Z(x_0) + x_0 f(x_0))}$, $x_0 = \left[l \dfrac{L_0}{Lk} \right]^{1/k} \sigma_u$, σ_u is the

mean strength of a wire, and $f_Z(x_0)$ is a Weibull probability density function.

Using the data of the tensile strength tests of 30 wires conducted by Faber et al. (2003) as an example, the mean value of the wire specimen strength σ_u=1788.7 MPa, the Weibull parameter k=72.62, and the scale factor is assumed to be λ=1, 3 and 10. The reduction curves for the mean strength of a cable system composed of 10 to 300 wires are shown in Fig. 2.
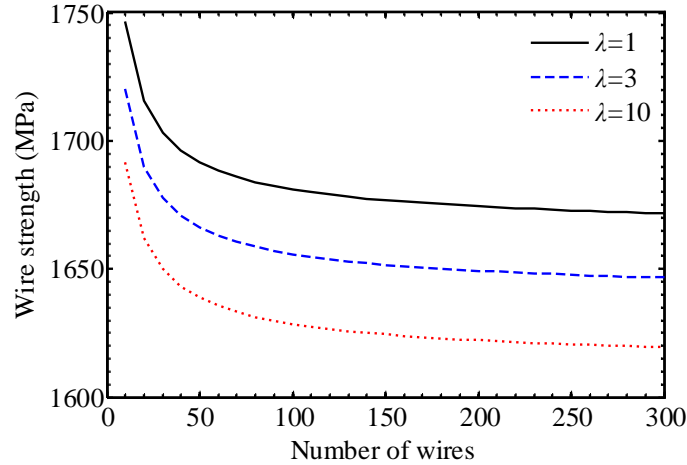

Fig. 2. Wire strength in a stay cable impacted by the number of wires

It is observed from Fig. 2 that the wire strength decreases rapidly with the initial increase in the number of wires. The increase in the number of wires from 10 to 300 leads to a 4.3% reduction in the wire strength. In addition, the wire strength decreases with a larger scale factor or a smaller correction length will reduce the wire strength. The deviation due to the Daniels effect is negligible, similar to the length effect.

2.2 Effect of fatigue-corrosion

Since high stress cables are prone of corrosion (Yang et al. 2012), stay cables become rusty and fractured under long-term exposure to corrosion and cyclic stresses. Thus, cable corrosion is a common phenomenon in existing cable-supported bridges. The cable corrosion of cable wires takes different forms, including stress corrosion cracking, pitting, corrosion fatigue and hydrogen embrittlement, which lead to reductions in the strength and ductility of wires as well as reductions in the cable lifetime (Mahmoud 2007). This study considers cable degradation resulting from atmospheric corrosion and fatigue damage.

In the concept of fatigue damage accumulation, the wire with the shortest failure times is assumed to break first in the system. Subsequently, the stress is redistributed to the remaining wires. Therefore, the probability distribution function of the initial failure time is written as follows (Maljaars and Vrouwenvelder 2014):

$$F_N(N, \sigma_{eq}) = 1 - \exp\left[-\left(\frac{\sigma_{eq}}{r_c}\right)^\alpha \left(\frac{N}{K}\right)^{\frac{\alpha}{m}}\right] \qquad (3)$$

where σ_{eq} and N are the equivalent stress range and the number of stress cycles, respectively, and can be estimated considering actual traffic loads; α, m and K are unknown coefficients that can be estimated by experimental tests; $r_c = (cnA_0)^{-\frac{1}{\alpha}}$ where n is the number of wires of the specimen, A_0 is the cross sectional area of the wire, and c is an unknown parameter; $K = K_0 \sqrt{1 - \frac{m_s}{m_z}}$ where K_0 can be

estimated from experiments of wires with known a strength and stress, m_s and m_z are the mean stress and the mean strength, respectively. Note that since the resistance and loading scenario of the cables are related, the distribution may not be identically and independently approximated. The correlation analysis has been conducted in the system reliability analysis in the case study.

Based on Faber et al. (2003)'s assumptions, the parameters for the cable are $n=200$, $\sigma_u=1789$ MPa, $\lambda=3$ and$\lambda=200$ for non-corroded and corroded wires, respectively; the parameters for the loading are $N=1.5\times10^6$ cycles per year, $\sigma_{eq}=30$MPa. In addition, the estimated parameters in Eq. (2) are $m=1.50$, $\alpha=2.76$, and $K_0=1.19\times10^6$MPa. Degradation functions of the cable strength for the uncorroded cables and corroded cable are

$$y_1(t) = -1.5\times10^{-5}t^2 - 3.2\times10^{-3}t + 0.998 \tag{4a}$$

$$y_2(t) = -4.7\times10^{-4}t^2 - 2.4\times10^{-3}t + 0.996 \tag{4b}$$

where t is time in year. The uncorroded cable is associated with only fatigue damage, and the corroded cable is associated with both fatigue and corrosion. It is observed that the strength coefficients of the stay cable associated with fatigue and fatigue-corrosion effects during the 20-year service period are 0.928 and 0.751, respectively.

2.3 Probability modeling of cable strength

As mentioned before, Faber et al. (2003) presented the procedures for probability modeling for cable strength using Ultra Sonic inspections and experimental results.

However, these results are hypothetical, since the experimental data are mostly assumption. This study consider the actual strength of the specimens of 69 corroded wires and 13 uncorroded wires in the stay cables of a highway bridge in China (Li et al. 2012). The wire specimens of the cables on service for about 20 years were supposed to have a free length of 500 mm. The evaluated probability models of the wire specimen are shown in Fig. 3.
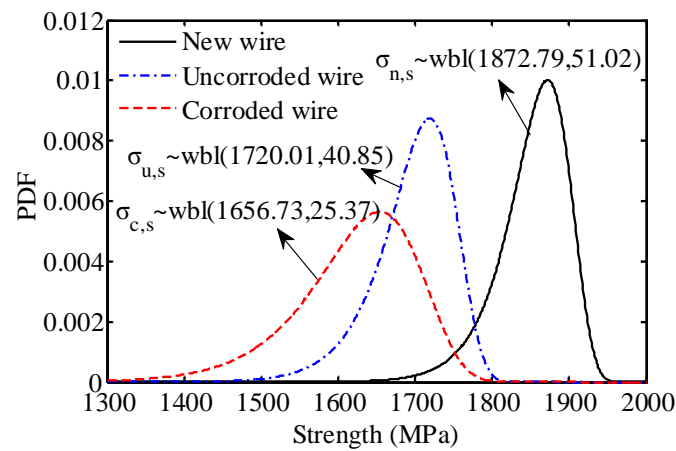

Fig. 3. Probability density of the strength of the specimen (Li et al., 2003)

In the present study, consider a stay cable with a length of 232 m that will be adopted in the following case study. The cable is consisted of n=243 parallel steel wires, and each wire has a diameter φ=7 mm. The design strength of the cable is 1766 MPa. Initially, the probability model of the strength of an individual wire is evaluated based on Eq. (2) and Fig. 3. The results are shown in Fig. 4.
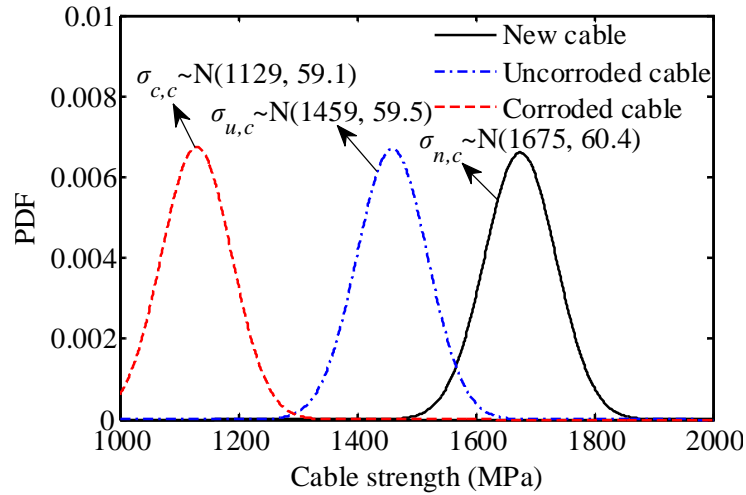
Fig. 4. Probability distribution of a prototype cable

As observed from Fig. 4, the mean value of the cable strength has decreased

by 32% and 13%, respectively. However, the standard deviation has decreased less

than 2%. The negligible of the deviation of the cable strength due to the cable

length effect and the Daniels effect is in agreement with Faber et al. (2003). Based

on the probability model of the prototype cable as shown in Fig. 4, the

time-variant probability model was evaluated considering the degradation function

shown in Eqs. (4). The time-variant degradation model of the cable in lifetime is
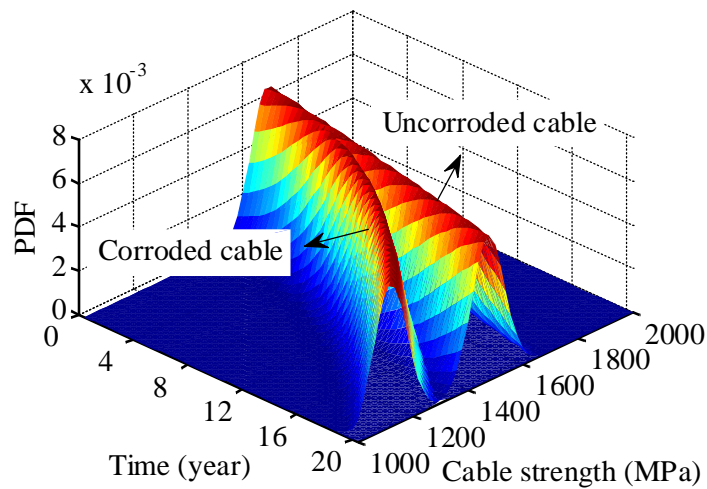
shown in Fig. 5.

Fig. 5. Time-variant probability densities of the cable strength

The degradation tendency of the cable strength shown in Fig. 5 is in accordance with the Faber et al. (2003), and the statistical parameters were referred to Li et al. (2003). It is observed that corrosion results in an accelerated reduction in the ultimate strength of a cable.

3 A computational framework for system reliability evaluation of cable-stayed bridges

Compared with common girder type bridges, a cable-stayed bridge exhibits unique characteristics such as the cable slag and beam-column effects and nonlinear behaviors (Freire et al. 2006). A cable-stayed bridge is a complex system consisting of multiple components connected in series or in parallel. These components work together as a system to support loading. Therefore, the system-level behaviors should be further considered in addition to the component-level behaviors illustrated above.

3.1 Component-level failure mode of a cable-stayed bridge

In general, the potential failure modes of a cable-stayed bridge are bending failure of towers and girders, strength failure of cables, and stability failure of pylons. This study concentrates on the simple failure model including bending failure and strength failure modes, while the stability failure mode is more complicated, which can be found in Cheng and Li (2009) and Zhang and Sun (2014). Compared with short-span girder bridges, long-span cable-stayed bridges exhibit nonlinear

behaviors under heavy traffic loading. The nonlinearities, including the cable sag effect, the beam-column effect and large displacement, should be considered in the formulation of the limit state functions.

For the strength failure of a stay cable, the long cable sag effect resulting from self-weight should be considered in nonlinear structural analysis. The conventional approach for considering this nonlinearity is Ernst's equivalent elastic modulus (1965). Large displacement of the girders also leads to nonlinear behavior in the stay cable. These nonlinearities can be considered in a time-history analysis in a finite element program and can be captured in a nonlinear limit state function:

$$Z_{Cable}^i = T_u^i(t) - T^i(X) \tag{3}$$

where Z_{Cable}^i is the limit state function for the strength failure of the ith cable, $T_u^i(t)$ is the time-variant wire strength of the ith cable and $T^i(X)$ is the service stress of the jth cable. The cable resistance term can be deduced from the models of the series-parallel system and the fatigue and corrosion effects, and the cable force term can be approximated by a learning machine with the samples simulated by finite element analysis.

Another significant failure mode for cable-stayed bridges is the bending failure of girders and pylons. Due to the high stress in stay cables, the beam-column effect is a unique factor impacting the mechanical behavior of the beams and pylons, especially in their bending failure state. In fact, the relationship

between bending moment and axial force will affect the component stiffness coefficient and the internal forces. The beam-column interaction is a second-order effect and can be conveniently considered by utilizing stability functions (Yoo et al. 2010). Assuming a hollow rectangular section, where the neutral axis in the ultimate state within the webs, the axial bending interaction curve can be evaluated via a sample plastic analysis and is written as follows (Yoo et al. 2012):

$$\frac{M}{M_P} = 1 - \left(\frac{P}{P_P}\right)^2 \frac{A^2}{4wZ_x} \tag{4}$$

where M is the applied moment, M_P is the plastic moment capacity in the absence of axial loads, P is the applied axial force, P_P is the plastic axial force capacity in the absence of applied moment, w is the web thicknesses, and Z_x is the bending plastic modulus. The beam-column effect can also be captured by a learning machine, which will be described later in detail.

3.2 System-level failure sequences and subsystem updating

Since a cable-stayed bridge is a statically indeterminate system composed of girders, cables and pylons, the failure of a component will result in the redistribution of the stress and strain within the system. If the structural subsystem still has the capacity to withstand the load, more and more components will fail with increases in the load. Finally, the structure becomes an unstable or a mechanism system, and the structure will collapse or fail to meet a requirement. In the above procedures, the system reliability can be modeled by combining the

failed components into a parallel system that forms a critical failure sequence and by combining the failure sequences into a series system. In this area, the conventional approaches of identifying the failure sequences are associated with the selecting and searching method. One of the technologies used to search for potential failure components is the branch-and-bound method known as the β-unzipping method (Liu et al. 2014).

The β-unzipping method utilizes the reliability index of each component to search for potential failure components. The removing of each potential failure component branches the initial structure into different substructures. The connection of the identified failed components into a parallel system forms a failure sequence that is similar to a zipper. Therefore, the searching procedure is actually an unzipping process. Suppose a system composed of n components, where k-1 components (denoted as r_1, r_2,…, r_{k-1}) failed. The conditional reliability index of the kth component is written as follows (Thoft-Christensen and Murotsu 1986):

$$\beta_{r_k/}^{(k)} = \beta_{r_k/r_1,r_2,\cdots r_{k-1}}^{(k)} = \Phi^{-1}\left[P(E_{r_k/}^{(k)})\right] \tag{5}$$

where $E_{r_k/}^{(k)}$ is the event of the kth component failure at the kth failure phase, $P()$ denotes the probability of the event, $\Phi^{-1}()$ is an inverse cumulative distribution function, and $\beta_{r_k/r_1,r_2,\cdots r_{k-1}}^{(k)}$ is a conditional reliability index of the kth potential component at the kth failure phase. The condition to be the potential failure component is as follows (Liu et al. 2016b):

$$\beta_{r_k/}^{(k)} \leq \beta_{\min}^{(k)} + \Delta\beta \qquad (6)$$

where $\beta_{\min}^{(k)}$ is the minimum reliability index at the kth failure phase, and $\Delta\beta$ is the increasing interval of the reliability index. Thoft-Christensen and Murotsu (1986) suggested that $\Delta\beta$ can be treated as 3 during the first searching process and 1 for the latter processes, for the purpose of conducting an efficient searching and selecting scheme.

The most critical procedure in the β-unzipping method is to break the initial system into subsystems that is called system updating (Chen et al. 1995). System updating is associated with the failure mode of the potential component. In structural engineering, the conventional approach for system updating involves adding a plastic hinge at the failure position to account for bending failure. However, because a cable-stayed bridge has multiple different failure modes as illustrated above, special attention should be paid to the system updating. The following assumptions for system updating for cable-stay bridges can be referred from the previous studies (Bruneau 1992). Firstly, for a brittleness failure mode, such as a cable rupture, the subsystem can be updated by directly removing the failed component. Secondly, for a ductile failure mode, such as the bending failure of girders and pylons, the subsystem can be updated by adding a plastic hinge at the failure location. The system failure of a cable-stayed bridge can be determined by the load-carrying capability of the entire structure or any other criterion, such as the serviceability.

In summary, the β-unzipping process is described as follows. Firstly, conduct a component-level reliability analysis for each structural element, then choose the minimum reliability index $\beta_{\min}^{(i)}$. Secondly, select the potential failure components with the reliability index in the interval [$\beta_{\min}^{(i)}, \beta_{\min}^{(i)} + \Delta\beta$]. Thirdly, branch the initial system into different subsystems according to the system updating criterion by separately removing the identified failed components. Fourthly, repeat the above procedures until the structure collapses or fails to meet a specified requirement. Finally, combine these reliability indices of identified components into a parallel-series system that is similar to an event tree, where the system reliability can be eventually evaluated.

As observed from the above deduction, the beam-column effect is considered in Eq. (3), and the failure sequence searching criteria is shown in Eqs. (4, 5). In addition to these unique characteristics illustrated above, the cable degradation will add to the time-consuming computation of the system reliability. Therefore, special attention should be paid to utilize an efficient computational framework.

3.3 Structural system reliability evaluation via machine learning

Due to the characteristics and cable degradation of the cable-stayed bridge, an efficient framework should meet the following requirements. Initially, the computing accuracy is an essential requirement, because the components have nonlinear mechanical behavior and extremely low failure probability. On this issue, the conventional first-order-second-moment (FOSM) approach cannot capture the

structural nonlinear behavior, and the conventional second-order response surface method (RSM) is incapable of capturing the structural higher-order nonlinear behavior (Liu et al. 2015; Alibrandi et al. 2015). Subsequently, since searching for the dominant failure sequence is a time-consuming process, computational efficiency is another essential requirement. Based on the above formulations, this study utilized a machine learning approach based on the adaptive support vector regression (ASVR) approach proposed by Liu et al. (2016a). The framework of the intelligent algorithm was improved for the special application of taking into account the cable degradation. The flowchart of the framework is shown in Fig. 6.
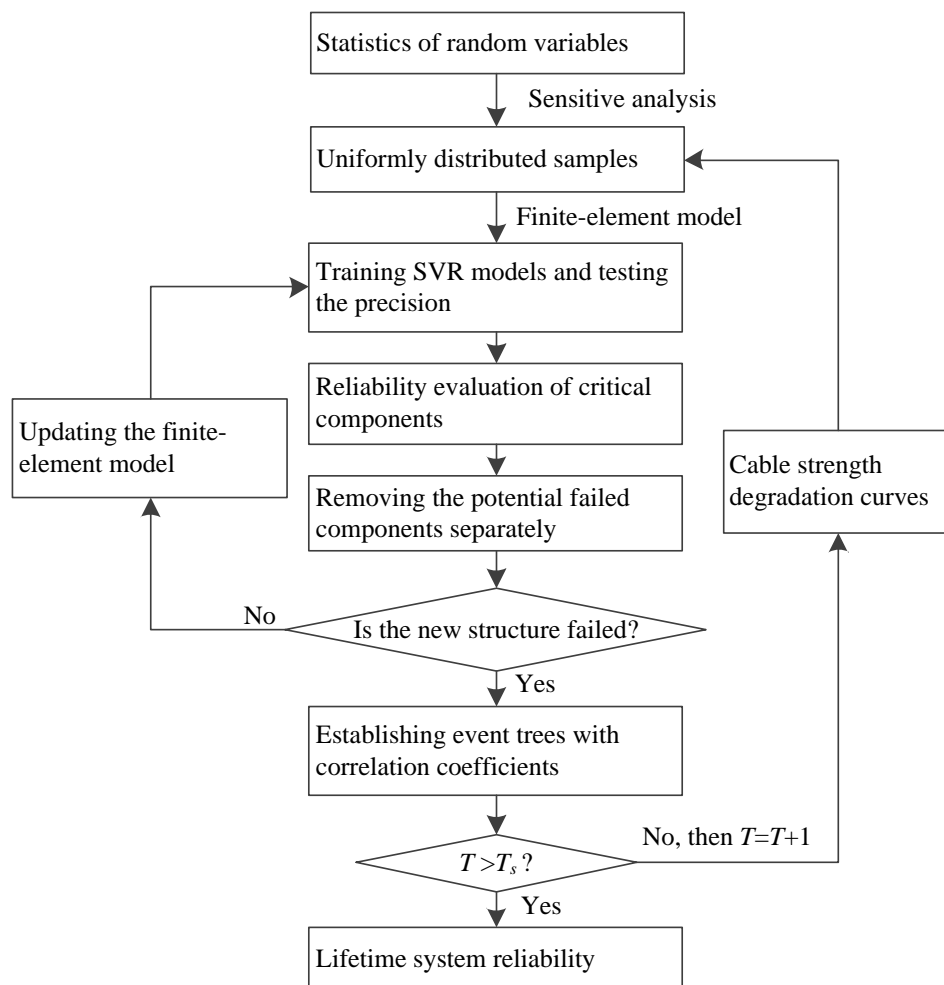
Fig. 6. Flowchart of the proposed ASVR approach

As depicted in Fig. 6, the main procedures in the flowchart consist of two aspects including the system reliability evaluation based on the ASVR approach and the updating of the cable degradation model. Details of the applications of the support vector regression (SVR) and ASVR approaches in structural system reliability evaluation can be found in Dai et al. (2012) and Liu et al.(2016b). This article mainly describes the procedures associated with cable degradation. Initially, the cable strengths are taken as initial values to carry out the system reliability evaluation step by step. Subsequently, the cable strength model is updated, and the component and system reliability is then reevaluated. It is worth noting that the event tree should be rebuilt when the cable strength changes, because cable degradation may change the potential failed components comprising the failure sequence. Finally, if the service period, T_s, is reached, the entire procedures will stop and will output the lifetime system reliability indices. The cable degradation-induced decrease in the system reliability will be reflected by the time-variant system reliability indices.

The critical step depicted in Fig. 6 is resampling the training samples after the cable strength is updated. This procedure suggests that it is inappropriate to only update the reliability index of individual cables without the reevaluation of the failure sequences. Instead, the seemingly additional computational effort is essential to capture the main failure sequences. Such deduction will be demonstrated in the case study.

As mentioned above, the introduction of the cable degradation leads to additional computational efforts. To make the computation more efficient, a graphical user interface (GUI)-based program entitled "Complex Structural Reliability Analysis software V 1.0" (CSRA) (2013) was developed based on the framework. This general program is based on two commercial programs, namely, MATLAB and ANSYS. The main procedures of the CSRA program are summarized in Fig. 7.
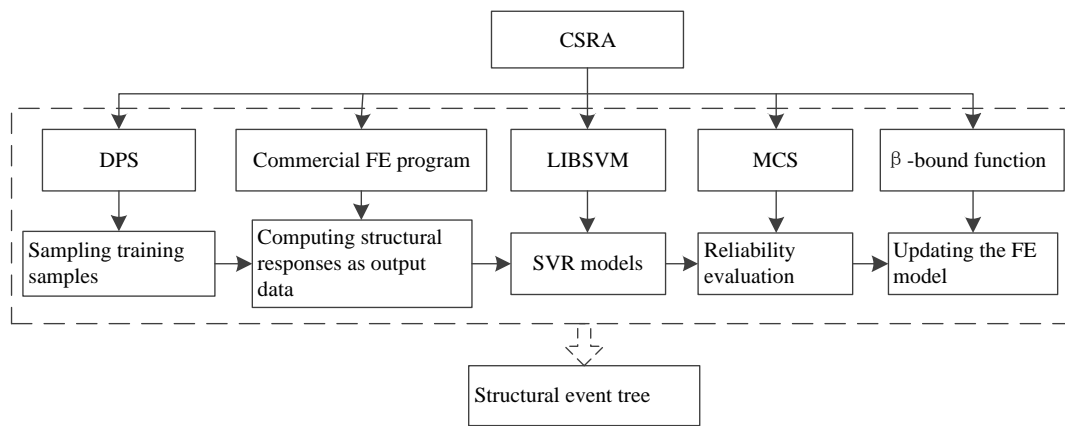

Fig. 7. Flowchart of the complex structural reliability analysis program

In Fig. 7, the Data Processing System (DPS) (Tang and Zhang 2013) is utilized to generate uniformly distributed samples that will be used for training SVR models. The LIBSVM (Library for Support Vector Machines) (Chang and Lin 2011) is an MATLAB program package. The MCS (Monte Carlo Simulation) can be a direct MCS or an importance sampling. The β-bound function refers to Eqs. (4) and (5). At the end of the procedure, the finite-element model is updated, and the component reliability is then reevaluated step by step. Eventually, the system reliability can be evaluated in a series-parallel system.

4 Case study of a short-span cable-stayed bridge

An ancient short-span cable-stayed bridge shown in Fig. 8 is presented to investigate the influence of cable degradation on the structural system reliability. The cable-stayed bridge has a single pylon and two stay cables on each side. The distance between the cable anchors in the girders is 30 m. More details regarding the material and section properties and performance functions can be found in Bruneau (1992). In this case study, the structural mechanical behavior is assumed to be linear and elastic in accordance with the results provided by Bruneau (1992).
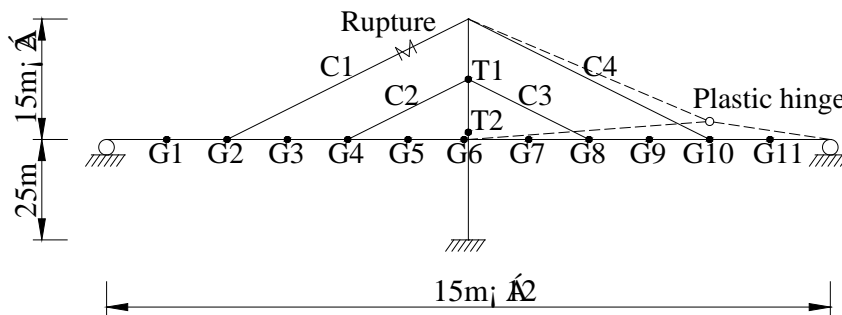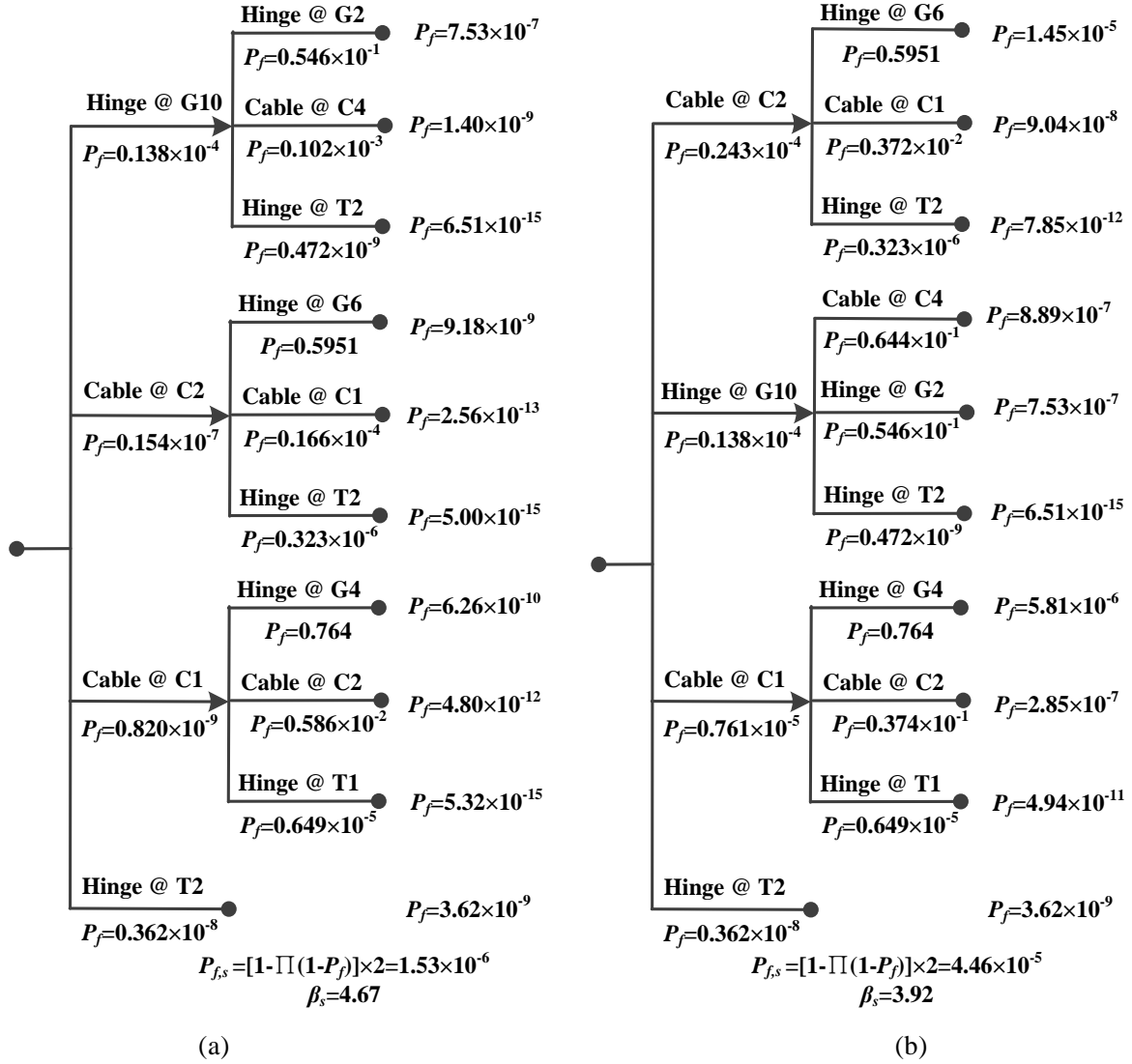

Fig. 8. Dimensions and failure modes of a short-span cable-stayed bridge

In general, the cables are considered brittle because the rupture of a stay cable is transient. The concrete girders and towers in long-span bridges are considered ductile because the prestressed structures are allowed to have large deflections. The structural system failure was defined by a plastic collapse mechanism. The plastic failure mechanism was identified by the plastic-hinge locations and plastic capacities. The potential failure locations are shown in Fig. 6. The points G1~G11 of the girders and the points of T_1 *and* T_2 of the pylon are critical to bending failure, and the points C1~C4 of the stay cables are critical to

sudden rupture.

In the system-level point of view, if the cable is ruptured, the substructure can be updated by removing the ruptured cables directly. If bending failure of a girder or a pylon occurs, a plastic hinge can be added to the location where the bending failure occures. It is acknowledged that the structural stiffness and resistance can change at any step, which means that the remaining structural elements will form a new structural system. At the end of the processes, the progression along the failure sequences will stop when the failure probability of the final component is expected to be extremely high. A two-level event tree was adopted by Breaneau (1992) to descript the partical event for the cable-stayed bridge. In the present study, the cable strength coefficients shown in Fig. 2 were utilized to update to the limit state functions provided by Breneau (1992). Based on the above assumptions, the event trees of the bridge system accounting for no degradation and a degradation coefficient of 20% were evaluated, as shown in Figs. 9.

Left tree (a):

Hinge @ G2
P_f=0.546×10⁻¹ → P_f=7.53×10⁻⁷

Hinge @ G10
P_f=0.138×10⁻⁴

Cable @ C4
P_f=0.102×10⁻³ → P_f=1.40×10⁻⁹

Hinge @ T2
P_f=0.472×10⁻⁹ → P_f=6.51×10⁻¹⁵

Hinge @ G6
P_f=0.5951 → P_f=9.18×10⁻⁹

Cable @ C2
P_f=0.154×10⁻⁷

Cable @ C1
P_f=0.166×10⁻⁴ → P_f=2.56×10⁻¹³

Hinge @ T2
P_f=0.323×10⁻⁶ → P_f=5.00×10⁻¹⁵

Hinge @ G4
P_f=0.764 → P_f=6.26×10⁻¹⁰

Cable @ C1
P_f=0.820×10⁻⁹

Cable @ C2
P_f=0.586×10⁻² → P_f=4.80×10⁻¹²

Hinge @ T1
P_f=0.649×10⁻⁵ → P_f=5.32×10⁻¹⁵

Hinge @ T2
P_f=0.362×10⁻⁸ → P_f=3.62×10⁻⁹

$P_{f,s} = [1-\prod(1-P_f)]\times2=1.53\times10^{-6}$
$\beta_s=4.67$

(a)

Right tree (b):

Hinge @ G6
P_f=0.5951 → P_f=1.45×10⁻⁵

Cable @ C2
P_f=0.243×10⁻⁴

Cable @ C1
P_f=0.372×10⁻² → P_f=9.04×10⁻⁸

Hinge @ T2
P_f=0.323×10⁻⁶ → P_f=7.85×10⁻¹²

Cable @ C4
P_f=0.644×10⁻¹ → P_f=8.89×10⁻⁷

Hinge @ G10
P_f=0.138×10⁻⁴

Hinge @ G2
P_f=0.546×10⁻¹ → P_f=7.53×10⁻⁷

Hinge @ T2
P_f=0.472×10⁻⁹ → P_f=6.51×10⁻¹⁵

Hinge @ G4
P_f=0.764 → P_f=5.81×10⁻⁶

Cable @ C1
P_f=0.761×10⁻⁵

Cable @ C2
P_f=0.374×10⁻¹ → P_f=2.85×10⁻⁷

Hinge @ T1
P_f=0.649×10⁻⁵ → P_f=4.94×10⁻¹¹

Hinge @ T2
P_f=0.362×10⁻⁸ → P_f=3.62×10⁻⁹

$P_{f,s} = [1-\prod(1-P_f)]\times2=4.46\times10^{-5}$
$\beta_s=3.92$

(b)

Figs. 9. Two-level event trees of the short-span cable-stayed bridge: (a) without cable degradation; (b) with a cable degradation coefficient of 20%

The following conclusions can be deduced from Figs. 7. First, the dominant failure sequence of the initial bridge is the Hinge @ G10 followed by the Hinge @ G2. However, the cable degradation shifts of the dominant failure to the Cable @ C2 followed by the Hinge @ G6. Secondly, a 20% reduction in the cable strength results in a rapid increase in the failure probability of the C2 cable from 0.154×10^{-7} to 0.243×10^{-4}. Finally, the decrease of the cable reliability results in the structural system reliability decrease from 4.67 to 3.92. In conclusion, the cable

degradation not only decreases the reliability of a cable but also has a significant impact on the structural dominant failure mode and the system reliability.

To investigate the lifetime degradation of the cable strength on the system reliability of the bridge, the system reliability was reevaluated based on the framework shown in Fig. 6. Fig. 10 plots the results of the time-variant system reliability of the bridge over a 20-year service period.
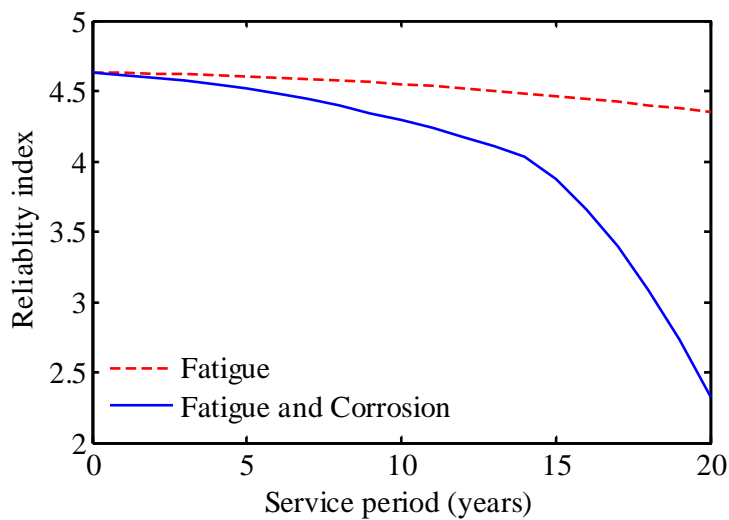

Fig. 10. System reliability of the short-span bridge subject to cable degradation

It is observed from Fig. 10 that the system reliability indices have a similar tendency as the cable strength models shown in Fig. 2. The reliability index accounting for fatigue and corrosion decreases rapidly compared to that caused by fatigue. However, the fatigue-corrosion effect leads to a sudden decrease in the reliability index starting in the 13th year. This phenomenon can be explained by the event tree shown in Fig. 9, where the cable failure becomes the dominant failure mode as the cable strength decreases to a critical value. The failure probability of a cable due to fatigue-corrosion effect will be larger than that of the

hinge at the G10 point from the 13th-year of service period. It can be derived that the continuous cable degradation has resulted in a transformation of the domain failure component from the girder to the cable, which leads to a sudden decrease in the system reliability index. However, this phenomenon is not observed in association with the fatigue-induced reliability decrease, because the cable strength has not decreased to the limit.

5 Case study of a long-span cable-stayed bridge

5.1 Prototype bridge

A long-span cable-stayed bridge (Liu et al. 2016a) crossing the Yangzi River in Sichuan province, China, is selected herein as a prototype to investigate the influence of cable degradation on the system reliability. The bridge has two pylons with double-sided cables forming a fan pattern. The pylon and segmental girders are connected by 34 pairs of cables on two sides. The dimensions of the bridge are shown in Fig. 11, where C_S^i and C_m^i denote the ith pair of cables in the side-span and the mid-span, respectively; G_S^j and G_S^j denotes the jth pair of girders in the side-span and the mid-span sides, respectively; and P_1, P_2 and P_3 denote the critical bending failure points of the pylon and the girder.
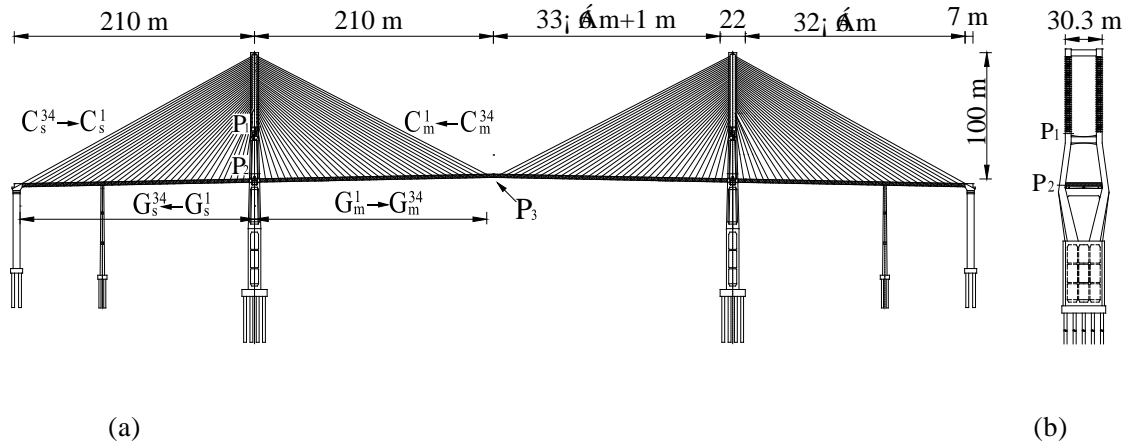
Fig. 11. Dimensions of the cable-stayed bridge: (a) elevation view; (b) side view

The diameter of a single parallel steel wire is φ=7 mm, and the physical properties of the wire were taken from the specifications of MOCAT (2010). The modulus of elasticity of the cables was estimated via Ernst's equation (Ernst, 1965). The physical properties of the four longest cables are shown in Table 1, where N_s is the number of wires in a stay cable. Design values of the parameters of the long-span cable-stayed bridge are shown in Table 2. The four-lane vehicle load was simplified as a uniform load on the mid-span girders following a normal distribution with the mean value of 63.5 kN/m and the standard deviation of 6.35. The purpose of the case study is to demonstrate the effective of the proposed computational framework and to investigate the influence of cable degradation on the system reliability of long-span cable stayed bridges.

Table 1. Physical properties of the four longest stay cables

Cables	N_s	A_s (m²)	$E_{s,\mathrm{Ernst}}$ (MPa)	T_0 (kN)
C_s^{34}, C_m^{34}	253	9.73×10^{-3}	1.864×10^5	6440
C_s^{33}, C_m^{33}	241	9.28×10^{-3}	1.860×10^5	6066

C_s^{32}, C_m^{32}	241	9.28×10^{-3}	1.852×10^5	5665
C_s^{31}, C_m^{31}	223	8.58×10^{-3}	1.841×10^5	5580

Table 2. Design values of the parameters of the long-span cable-stayed bridge

Variable	Mean value	Description
E_c	3.45×10^4 MPa	Modulus of elasticity of the concrete
$E_{s,Ernst}$	Table 1	Equivalent modulus of elasticity of the stay cable
γ_c	26 kN/m^3	Density of the concrete
γ_s	78 kN/m^3	Density of the steel cable
A_{c1}	20.8 m^2	Cross-sectional area of the girder
A_{c2}	26.8 m^2	Cross-sectional area of the pylon
A_s	*Table 2*	Cross-sectional area of the cable
f_s	1770 MPa	Initial ultimate strength of the steel cable
$f_{ck,d}$	23.1MPa	Design value of the ultimate compressive strength of the concrete
I_1	18.598 m^4	Inertia moment of the girder
I_2	118.4 m^4	Inertia moment of the pylon
Q	63.5 kN.m^{-1}	Vehicle load on the girders in mid-span

5.2 Deterministic analysis

Deterministic analysis of the bridge was conducted via a finite element model in

ANSYS, as shown in Fig. 12, where the cables were simulated by LINK180

elements and the girders and pylons were simulated by BEAM188 elements. The

traffic load was treated as uniformly distributed forces on the mid-span girders.

The critical failure components were the longest cables according to Liu et al.

(2016a). Taking the C_m^{31}, C_m^{32} and C_m^{33} cables and the P_1, P_2 and P_3 girders as examples, their dynamic responses under the sudden failure of the C_m^{34} cable are shown in Fig. 13. As observed from Fig. 13, both the cable forces and the bending moments increase rapidly following the sudden rupture of a stay cable. This phenomenon leads to the vibration of these components, which weaken over time.
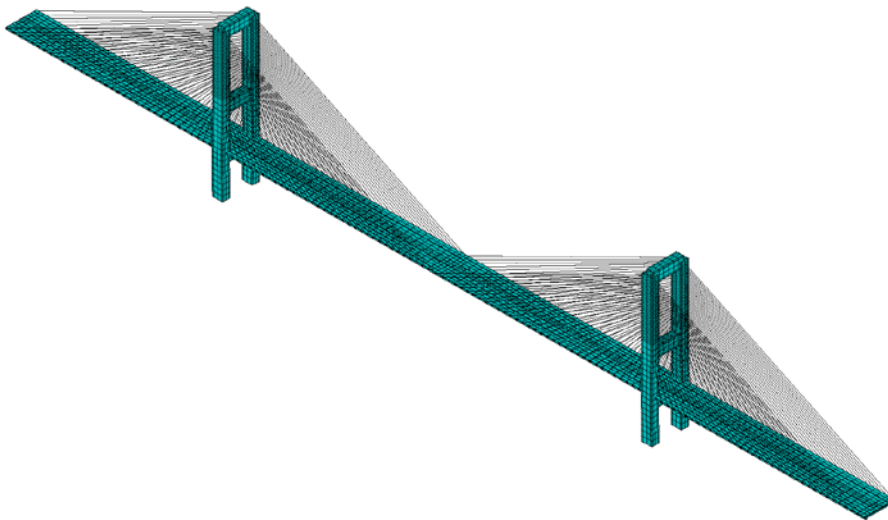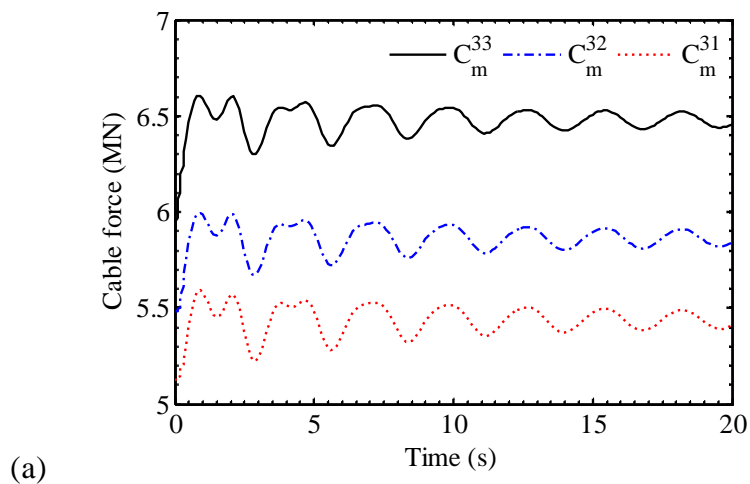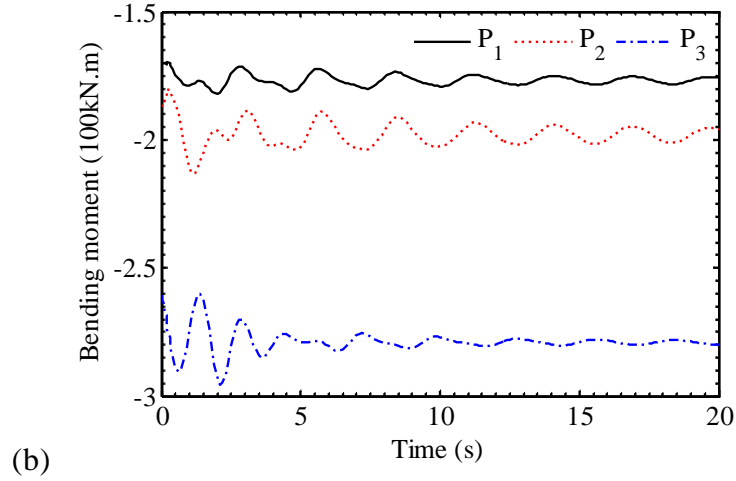

Fig. 12. Finite element model of the cable-stayed bridge

(a)

(b)

Figs. 13. Response histories of the critical points subjected to sudden rupture of the C_m^{34} cable: (a) cable force; (b) bending moment

Comparison between the static and dynamic increase rates of the critical components (indicated as δ_s and δ_d, respectively) due to the cable C_m^{34} failure are summarized in Table 3. It is observed that the component close to the ruptured cables has a larger increase rate. The static increase rate for the cable force (Cm33) and the maximum bending moment (P3) are 7.12% and 6.46%, respectively. The dynamic increase rate for the maximum cable force and the maximum bending moment of the girder are 11.10% and 11.79%, respectively. This phenomenon indicates that the dynamic effect due to a cable failure is non-ignorable.

Table 3. Increase rates of critical internal forces subjected to C_m^{34} rupture

| Component	C_m^{33}	C_m^{32}	C_m^{31}	P_1	P_2	P_3
δ_s	7.12%	6.55%	6.05%	3.53%	4.84%	6.46%
δ_d	11.10%	9.29%	8.01%	7.65%	11.05%	11.79%

Before utilizing the response data to approximate response functions, a parametric study was conducted to identify the most sensitive structural parameters with respect to the maximum response. The parameters in Table 1,

except for the resistance terms of f_s and f_{ck}, were selected for the parametric sensitive study. The sensitive values were evaluated by the following steps: (1) evaluate the response of a bridge element (defined as a_0) considering the mean value of all random parameters; (2) reevaluate the response of the bridge element (defined as a_i) considering increasing the value of the ith random variable by 10% and keeping the other parameters as the same; (3) repeat the second step to compute every a_i; (4) the sensitive value for the ith random variable is

$s_i = \dfrac{a_i - a_0}{\sum\limits_{i=1}^{n}(a_i - a_0)^2}$. The sensitive values of each parameter with respect to the cable

force and the bending moment of the girder are shown in Fig. 14.

(a)

(b)
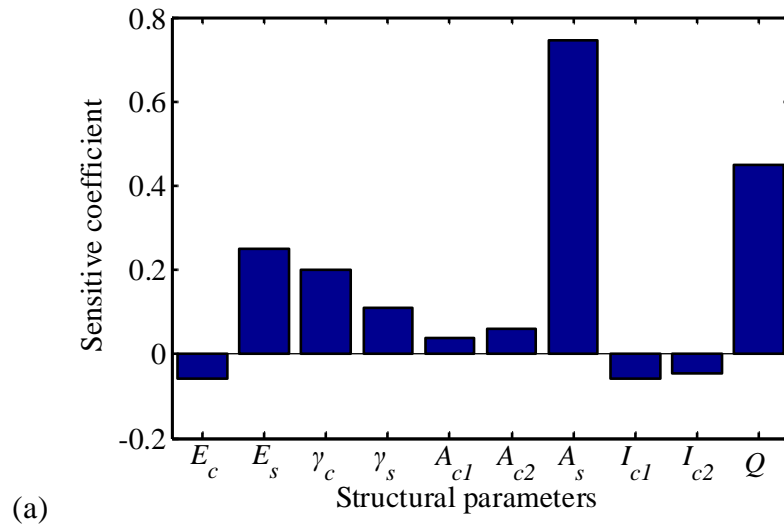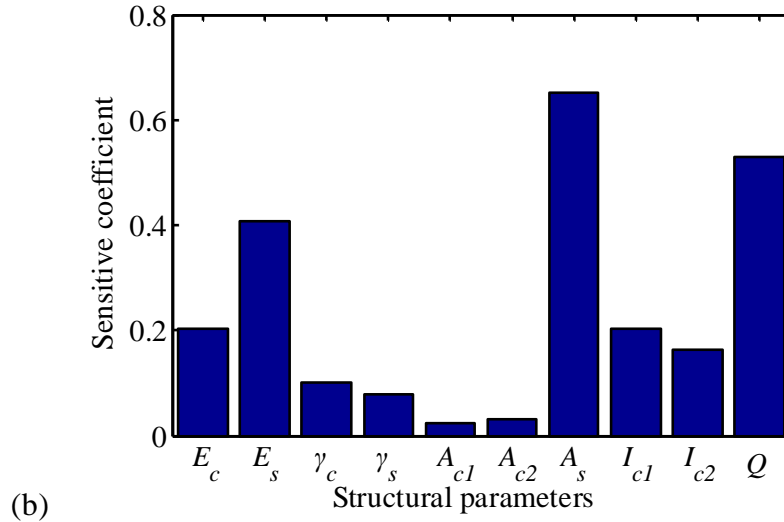
Figs. 14. Sensitive values of the structural parameters on: (a) C_m^{33} cable force; (b)P3 bending moment

It is observed that the most sensitive four parameters are A_s and Q, followed by E_s and γ_c. Therefore, the above-mentioned parameters were selected as random variables for structural reliability analysis. In addition, A_s and E_s values were assigned following a lognormal distribution with a coefficient of variation (COV) of 0.05, γ_c was assigned following a normal distribution with a COV=0.1, and Q was assigned following a Gumbel distribution with a COV=0.1.

In the learning machine, the input data are the uniformly distributed samples composed of A_s, E_s, γ_c and Q, and the output data are the maximum value in the response history, as shown in Fig. 15. A uniformly design scheme with 20 samples in a DPS program (Tang and Zhang 2013) was adopted. The response surfaces of the critical components in the initial structure or the updated structure were approximated via the learning machine considering dynamic effects. Fig. 13 shows the response surfaces of the C_m^{34} cable force, where Q and A_s were considered as variables and E_s and γ_c were considered as constants.
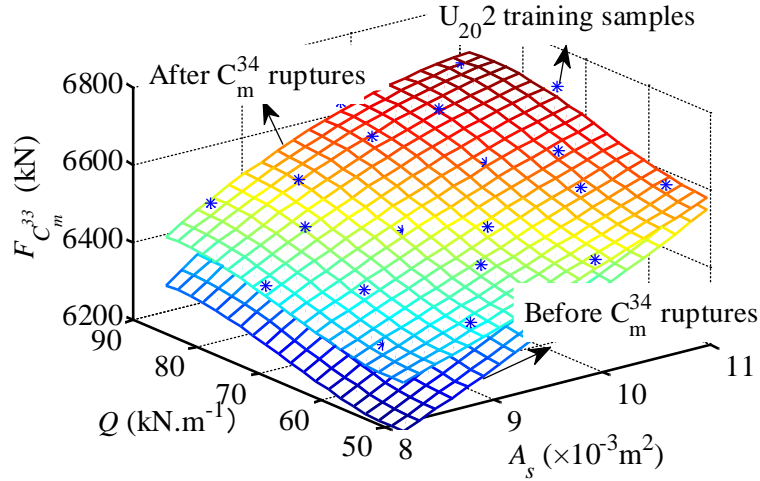
Fig. 15. Response surfaces of the C_m^{33} cable force subjected to the C_m^{34} rupture

It is observed that the training samples are uniformly distributed in the space, and the response surface fits the training samples fairly good. The response surface is nonlinear because of the dynamic effect and the nonlinear behavior of the structure. In addition, the C_m^{34} failure leads to an evident shift of the response surface, which has been captured by the support vector updating. With the explicit response surfaces, the component reliability can be evaluated via the first-order reliability method or the MCS.

5.3 System reliability evaluation

The system failure for the cable-stayed bridge was considered the bending failure of any girders or pylons. Therefore, the bending failure at points P_1 and P_2 on the pylon and the bending failure at point P_3 on the girder were considered aspects of the system failure. Since there are 34 pairs of cables on each side of the pylons and they are highly correlated, only the longest cables of C_m^{34} and C_s^{34} were selected as the first layer of the event tree. Two event trees for $T=0$ year and $T=20$ years

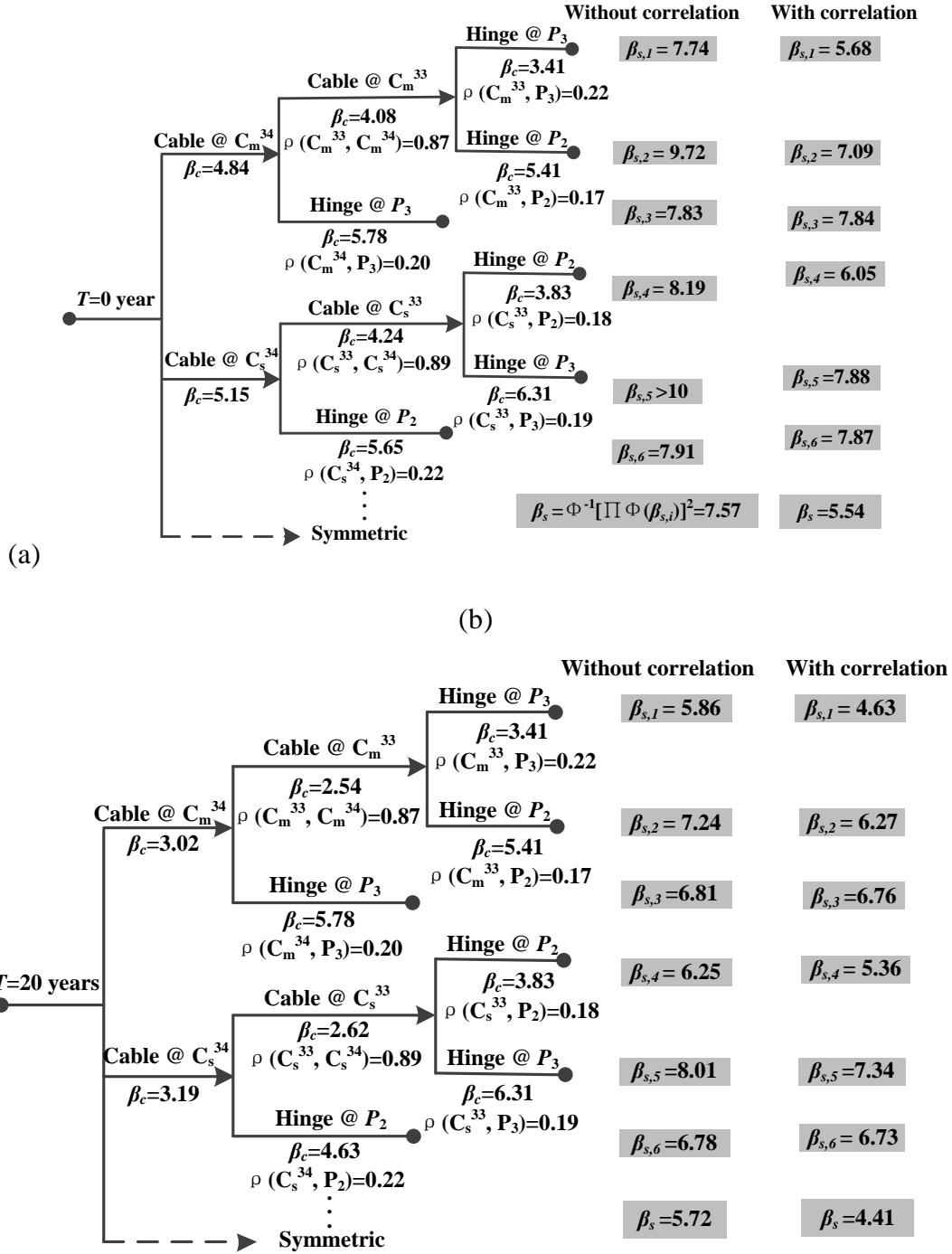were constructed as shown in Figs. 16 via the β-unzipping approach.

(a)

(b)

Fig. 16. Three-level event trees of the long-span cable-stayed bridge at: (a) T=0 year; (b) T=20 years

In Figs. 16, β_c is a component reliability index evaluated from the corresponding SVR model, $\beta_{s,i}$ is a system reliability index of the ith failure path with β_c in parallel, β_s is the system reliability index that is composed of $\beta_{s,i}$ in

series, and ρ is the correlation coefficient between two failure components.. It is observed from the event tree that there are two dominant failure paths. The first failure path is the strength failure of the mid-span cables (C_m^{34} and C_m^{33}) followed by the bending failure of the mid-span girder (Hinge @ P_3). The second failure path is the strength failure of the side-span cables (C_s^{34} and C_s^{33}) followed by the bending failure of the pylons (Hinge @ P_2). In this case study, the cable degradation did not change the domain failure path over the cable lifetime. This phenomenon can be explained by the fact that long-span cable-stayed bridges have dense cables providing large degrees of redundancy that can avoid the bending failure of the bridge girder. Therefore, the cable degradation or a cable loss will not change the domain failure mode from the cable failure to the girder failure. It can also be inferred that the cable strength degradation has a greater effect on the system safety of a cable-stayed bridge with long-spacing (e.g. 30 m) cables compared to that of the short-spacing (e.g. 6 m) cables.

The correlation coefficients in the event trees were evaluated based on their response surface functions. According to the concept of the probability network estimating technique (PNET) (Ang, 1984), the components can be classified based on their correlation coefficients. In general, the components with correlation coefficients larger than a threshold coefficient, i.e., approximately 0.8 (Liu et al. 2014), can be simplified as a representative component; otherwise, the two components can be considered independently. In the first failure path shown in Fig.

14, ρ ($C_m{}^{34}$ and $C_m{}^{33}$) = 0.87, higher than the demarcating coefficient; ρ ($C_m{}^{34}$ and $C_m{}^{33}$) = 0.22, lower than the demarcating coefficient. As a result, the consideration of the correlation effect leads to the reliability of the failure path $\beta_{s,1}$ decreases from 7.76 to 5.68. This phenomenon results from the highly correlated cable strength and response models, which reduce the number of independent components in a parallel failure path. Thus, without consideration of correlation between two failure modes will provide a non-conservative result.

The target system reliability index β_T is chosen herein as a reference to evaluate the scheme for cable replacement. The MOCAT in China (1999) recommends β_T = 5.2, and the AASHTO (2004) recommends β_T =5.0~6.0, as suggested by Nowak (2000). The lifetime system reliability of the cable-stayed bridge considering correlation was reevaluated as shown in Fig. 17, where T_L is the design lifetime of a cable. As observed from Fig. 17, the service time of the bridge corresponding to β_T = 5.0 for the bridges with uncorroded and corroded cables are approximately 28 and 12 years, respectively.
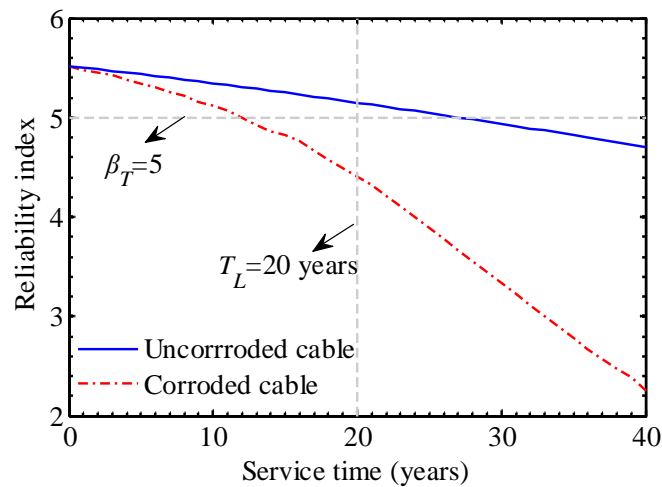
Fig. 17. System reliability of the cable stayed bridge subjected to cable degradation

It can be inferred from the case study that the cable failures in the event tree are highly correlated, contributing to an evident decrease in the system reliability. Although the high degree of redundancy in a cable-stayed bridge contributes to the system safety of a cable-stayed bridge, highly corroded and correlated cables will reduce the system safety of the bridge. Therefore, the consideration of cable corrosion and correlation is important for lifetime safety evaluation of in-service cable-stayed bridges. A father analysis based on the proposed computational framework and site-specific cable inspection data can provide a theoretical basis for cable replacement.

6 Conclusions

A computational framework is proposed to evaluate the system reliability of cable-stayed bridges subjected to cable degradation. This framework can be applied as a general tool to any cable-supported bridge considering cable degradation. It advances the state of the art by capturing the influence of cable strength reduction on the bridge system reliability over the bridge lifetime. The effects of corrosion and correlation between defects were considered in the strength reduction model.

The case studies of two cable-stayed bridges, including an ancient short-span bridge with long cable spacing (30 m) and a modern long-span bridge with short cable spacing (6 m), have demonstrated the influence of the cable degradation on the structural system reliability. Several critical factors affecting the bridge

lifetime safety were found from the case study. The conclusions are summarized as follows.

(1) The cable strength reduction due to fatigue-corrosion effect over the cable lifetime can be up to 25%, and the dynamic amplification factor of the load effect resulting from a cable rupture can be as high as 11%. These features and the structural nonlinear behavior have been captured by updating the learning machines in the proposed computational framework.

(2) The cable strength degradation due to fatigue-corrosion effect can change the dominant failure path of a cable stay bridge, and thereby leads to a significant reduction in the bridge system reliability. This phenomenon is associated with cable spacing, where a sparse cable system seems more sensitive to the cable strength reduction and the dense cable system is relatively less sensitive to the cable degradation.

(3) In addition to the cable degradation, the strong correlation in cable defects also leads to a reduction in the system safety. Although a cable-stayed bridge has a high degree of redundancy that contributes to the system safety, strongly corroded cables with high correlation in the damage reduces the system safety of the bridge.

(4) For a target system reliability index of 5.0, the corresponding lifetime of the long-span cable-stayed bridge is 18 years. In order to extend this lifetime, the proposed framework provides a basis for targeted cable replacement in

conjunction with site-specific inspection data.

A better understanding of the cable degradation effect on the system reliability of cable-stayed bridges was provided by this study. However, the system reliability evaluation of cable-stayed bridges is a comprehensive task and can be improved further in the future: (1) a further analysis based on site-specific cable inspection data can provide a theoretical basis for deriving cable replacement schemes; (2) a complete event tree of the cable-stay bridge will be built for an in-depth investigation; and (3) the influence of the cable spacing on the structural system reliability deserves further investigation.

Acknowledgements

References

Vulnerability and Robustness of Corroded Large-Span Cable-Stayed Bridges under Marine Environment

Cheng, J., & Li, Q. S. (2009). Reliability analysis of a long span steel arch bridge against wind-induced stability failure during construction. Journal of

Constructional Steel Research, 65(3), 552-558.

Zhang, X., & Sun, H. (2014). Study of the aerostatic and aerodynamic stability of super long-span cable-stayed bridges. Engineering Sciences(2), 82-92.

Liu, Y., Lu, N., & Yin, X. (2016). A hybrid method for structural system reliability‐based design optimization and its application to trusses. Quality & Reliability Engineering International, 32(2), 595-608.

AASHTO. (2004). *AASHTO LRFD bridge design specifications*, Washington, DC.

ANSYS [Computer software]. ANSYS, Canonsbug, PA, USA.

Aoki, Y., Valipour, H., Samali, B., and Saleh, A. (2013). "A study on potential progressive collapse responses of cable-stayed bridges." *Adv. Struct. Eng.* 16(4), 689-706.

Bruneau, M. (1992). "Evaluation of system-reliability methods for cable-stayed bridge design." *J. Struct. Eng.*, 10.1061/(ASCE)0733-9445(1992)118:4(1106), 1106-1120.

Cao Y., Vermaas, G.W., Betti, R., West, A.C., Duby, P.F. (2003). "Corrosion and degradation of high-strength steel bridge wire." *Corrosion* 59(6), 547-554.

Chang, C.C., and Lin, C.J. (2011). "LIBSVM: a library for support vector machines." *ACM Transactions on Intelligent Systems and Technology (TIST)* 2(3), 27.

Cheng, J. Xiao, R.C. (2005). "Serviceability reliability analysis of cable-stayed

bridges." *Struct. Eng. Mech.* 20(6), 609-630.

CSRA [Computer software]. Complex Structural Reliability Analysis V 1.0, Changsha University of Science and Technology, Changsha, China

Dai, H., Zhang, H., Wang, W. (2012). "A support vector density-based importance sampling for reliability assessment." *Reliab. Eng. Syst. Safe.* 106, 86-93.

Daniels HE. (1945). The statistical theory of the strength of bundles of threads, Part I. *Proc Roy Soc, A* 183: 405–35.

Estes, A.C., and Frangopol, D.M. (2001). "Bridge lifetime system reliability under multiple limit states." *J. Bridge Eng.* 10.1061/(ASCE)1084-0702(2001)6:6(523), 523-528.

Faber, M.H., Engelund, S., and Rackwitz, R. (2003). "Aspects of parallel wire cable reliability." *Struct Safe* 25(2), 201-225.

Freire, A.M.S., Negrao, J.H.O., and Lopes, A.V. (2006). "Geometrical nonlinearities on the static analysis of highly flexible steel cable-stayed bridges." *Comput. Struct.* 84(31), 2128-2140.

Jia B., Yu X., Yan Q., Zhen Y. (2016). Study on the system reliability of steel-concrete composite beam cable-stayed bridge. *The Open Civil Engineering Journal.* 10(1):418-432

Kim, D.S., Ok, S.Y., Song, J., and Koh, H.M. (2013). "System reliability analysis using dominant failure modes identified by selective searching technique." *Reliab. Eng. Syst. Safe.*, 119, 316-331.

Lee, Y.J., and Song, J. (2011). "Risk analysis of fatigue-induced sequential failures by branch-and-bound method employing system reliability bounds." *J. Eng. Mech.* 10.1061/(ASCE)EM.1943-7889.0000286, 807-821.

Li W, Yan Q S, Wang W. (2010). System reliability analysis of cable-stayed bridge[J]. *Journal of Shenyang University of Technology*, 32(2):235-240. (in Chinese)

Li H., Li, S., Ou, J., Li, H. (2012a). "Reliability assessment of cable-stayed bridges based on structural health monitoring techniques." *Struct. Infrast. Eng.* 8(9), 829-845.

Li, H., Lan, C. M., Ju, Y., and Li, D. S. (2012b). "Experimental and numerical study of the fatigue properties of corroded parallel wire cables." *J. Bridge Eng.*, 17(2), 211-220.

Li, S., Xu, Y., Zhu, S., Guan, X., & Bao, Y. (2015). Probabilistic deterioration model of high-strength steel wires and its application to bridge cables. *Structure & Infrastructure Engineering, 11*(9), 1240-1249.

Xu, Y., Li, H., Li, S., Guan, X., & Lan, C. (2016). 3-d modelling and statistical properties of surface pits of corroded wire based on image processing technique. Corrosion Science, 111, 275-287.

Li, S., Xu, Y., Li, H., & Guan, X. (2014). Uniform and pitting corrosion modelling for high strength bridge wires. ASCE Jounal of Bridge Engineering, 19, 04014025. doi:10.1061/(ASCE)BE.1943-5592.0000598.

Liu, Y., Lu, N., Noori, M., and Yin X. (2014). "System reliability-based optimization for truss structures using genetic algorithm and neural network." *Int. J. Relia. Safe.* 8(1), 51-69.

Liu, Y. Lu, N., Yin, N. and Noori, M. (2016a). "An adaptive support vector regression method for structural system reliability assessment and its application to a cable-stayed bridge." *P. I. Mech O: J. Ris.*, 230(2), 204-219.

Liu, Y., Lu, N., and Yin, X. (2016b). "A hybrid method for structural system reliability-based design optimization and its application to trusses." *Qual. Reliab. Eng. Int.* 32(2), 595-608.

~~Lu, N., Liu, Y., Xiao, X., Yin, X. (2015). System reliability assessment of cable-stayed bridges based on a combined intelligent algorithm. Chinese Journal of Applied Mechanics, 32(5): 858-864. (in Chinese)~~

Mahmoud, K.M. (2007). "Fracture strength for a high strength steel bridge cable wire with a surface crack." *Theor Appl Fract Mec* 48(2), 152-160.

Maljaars, J., and Vrouwenvelder, T. (2014). "Fatigue failure analysis of stay cables with initial defects: Ewijk bridge case study." *Struct. Safe.* 51, 47-56.

MATLAB R2010b [Computing software]. MathWorks, Natick, MA.

Marjanishvili, S.M. (2004). "Progressive analysis procedure for progressive collapse." *J. Perform. Constr. Fac.* 18(2) 79-85.

Mehrabi, A. B., Ligozio, C. A., Ciolko, A. T., & Wyatt, S. T. (2010). "Evaluation, rehabilitation planning, and stay-cable replacement design for the hale boggs

bridge in Luling, Louisiana." J. Bridge Eng., 10.1061/(ASCE)BE.1943-5592.0000061, 364-372.

Ministry of Communications and Transportation (MOCAT). *Stay cables of parallel steel wires for large-span cable-stayed bridge JT/T 775-2010*, Beijing, China, 2010.

Ministry of Housing and Urban-Rural Development (MOHURD). (1999). *Unified standard for reliability design of highway engineering structures GB/T 50283-1999*, Beijing, China, 1999.

Mozos, C.M., Aparicio, A.C. (2010). "Parametric study on the dynamic response of cable stayed bridges to the sudden failure of a stay, Part I: Bending moment acting on the deck." *Eng. Struct.* 32(10), 3288-3300.

Mozos, C.M., Aparicio, A.C. (2011). "Numerical and experimental study on the interaction cable structure during the failure of a stay in a cable stayed bridge." *Eng. Struct.* 33 (8), 2330-2341.

Nakamura, S., and Suzumura, K. (2012). "Experimental study on fatigue strength of corroded bridge wires." *J. Bridge Eng.*, 10.1061/(ASCE)BE.1943-5592.0000366, 200-209.

Nowak, A.S., and Szerszen, M.M. (2000). Structural reliability as applied to highway bridges. *Progress in Structural Engineering & Materials*, 2(2), 218-224.

Stewart M.G., Al-Harthy A. (2008). Pitting corrosion and structural reliability of

corroding RC structures: Experimental data and probabilistic analysis. *Reliability Engineering & System Safety*, 93(3):373-382.

Thoft-Christensen, P., and Murotsu, Y. (1986). *"Application of structural systems reliability theory."* Speinger-Verlag Berlin, Heidelberg.

Tang, Q.Y., and Zhang, C.X. (2013). "Data Processing System (DPS) software with experimental design, statistical analysis and data mining developed for use in entomological research." *Insect Sci* 20(2), 254-260.

Weibull W. (1949).A statistical representation of fatigue failure in solids. Transactions on the Royal Institute of Technology. Stockholm, Sweden.

Wolff, M., Starossek, U. (2009). "Cable loss and progressive collapse in cable-stayed bridges." Bridge Structures 5(1), 7-28.

Xu, J., Chen, W. (2013). "Behavior of wires in parallel wire stayed cable under general corrosion effects." *J. Constr. Steel Res.* 85, 40-47.

Yang, W., Yang, P., Li, X., and Feng, W. (2012). "Influence of tensile stress on corrosion behaviour of high-strength galvanized steel bridge wires in simulated acid rain." *Mater Corros* 63(5), 401-407.

Yang, O., Li, H., Ou, J., and Li, Q. S. (2013). "Failure patterns and ultimate load-carrying capacity evolution of a prestressed concrete cable-stayed bridge: case study." *Adv. Struct. Eng.*, 16(7), 1283-1296.

Yoo, H., Na, H.S., Choi, E.S., and Choi, D.H. (2010). "Stability evaluation of steel girder members in long-span cable-stayed bridges by member-based stability

concept." *Int. J. Steel Struct.* 10(4), 395-410.

Yoo, H., Na, H.S., and Choi, D.H. (2012). "Approximate method for estimation of collapse loads of steel cable-stayed bridges." *J. Constr. Steel Res.*, 72, 143-154.

Zhou, Y. and Chen, S. (2014). "Time-progressive dynamic assessment of abrupt cable-breakage events on cable-stayed bridges." *J. Bridge Eng.* 10.1061/(ASCE)BE.1943-5592.0000517, 159-171.

Zhou, Y., Chen, S. (2015). "Numerical investigation of cable breakage events on long-span cable-stayed bridges under stochastic traffic and wind." *Eng. Struct.* 105, 299-315.

Zhu J, Wu J. (2011). Study on system reliability updating through inspection information for existing cable-stayed bridges. Advanced Materials Research, 250-253: 2011-2015.